www.nature.com/aps

Acta Pharmacologica Sinica

ARTICLE

Sortilin deletion in the prefrontal cortex and hippocampus ameliorates depressive-like behaviors in mice via regulating ASM/ceramide signaling

Shu-jian Chen[1], Cong-cong Gao[1], Qun-yu Lv[1], Meng-qi Zhao[1], Xiao-ying Qin[1] and Hong Liao[1]

Major depressive disorder (MDD) is a common psychiatric disorder characterized by persistent mood despondency and loss of motivation. Although numerous hypotheses have been proposed, the possible pathogenesis of MDD remains unclear. Several recent studies show that a classic transporter protein, sortilin, is closely associated with depression. In the present study, we investigated the role of sortilin in MDD using a well-established rodent model of depression. Mice were subjected to chronic unpredictable mild stress (CUMS) for 6 weeks. We showed that the expression levels of sortilin were significantly increased in the prefrontal cortex and hippocampus of CUMS mice. The depressive-like behaviors induced by CUMS were alleviated by specific knockdown of sortilin in the prefrontal cortex and hippocampus. We revealed that sortilin facilitated acid sphingomyelinase (ASM)/ceramide signaling, which activated RhoA/ROCK2 signaling, ultimately causing the transformation of dendritic spine dynamics. Specific overexpression of sortilin in the prefrontal cortex and hippocampus induced depressive-like behaviors, which was mitigated by injection of ASM inhibitor SR33557 (4 μg/μL) into the prefrontal cortex and hippocampus. In conclusion, sortilin knockdown in the prefrontal cortex and hippocampus plays an important role in ameliorating depressive-like behavior induced by CUMS, which is mainly evidenced by decreasing the trafficking of ASM from the trans-Golgi network to the lysosome and reducing the ceramide levels. Our results provide a new insight into the pathology of depression, and demonstrate that sortilin may be a potential therapeutic target for MDD.

Keywords: depression; sortilin; ASM/ceramide; RhoA/ROCK2; cofilin; dendritic spines; prefrontal cortex; hippocampus; SR33557

Acta Pharmacologica Sinica (2022) 43:1940–1954; https://doi.org/10.1038/s41401-021-00823-0

INTRODUCTION

Depression, a potentially devastating psychiatric disorder, has become a serious public health problem with high prevalence. Depression is estimated to affect over 16% of the global population, with an associated annual cost of over $200 billion [1]. However, available antidepression therapies are not sufficiently effective; almost one third of major depressive disorder (MDD) patients do not respond to these therapies, which significantly impedes the treatment of depressive disorders. Therefore, clarifying the detailed mechanisms underlying depression is an important public health goal [2].

Sortilin, a 95-kDa type-1 transmembrane protein, is widely expressed in many mammalian cell types in most tissues and highly expressed in neurons in the central nervous system (CNS) [3, 4]. After synthesis on the endoplasmic reticulum in precursor form, sortilin is trafficked to the trans-Golgi network (TGN) and then cleaved by the enzyme furin to its mature form [5, 6]. Mature sortilin is transported onto the cell membrane, where it functions as a receptor, binding with several proteins such as lipoproteins, neuropeptides [7, 8], and cytokines [9], or forming a co-receptor with p75NTR [7], GPCR, or ion channels [10] to mediate downstream signaling events. Mature sortilin can also combine with several adaptor proteins within cells to participate in the sorting and transport of numerous proteins such as neurotrophins [8], prosaposin [8], cathepsin D, cathepsin H [11], and progranulin [12] to contribute indirectly to other physiological or pathological processes. Numerous studies have shown that abnormal sortilin expression is closely associated with the onset and progression of many diseases, including hypercholesterolemia [13], obesity and insulin resistance [14, 15], Huntington's disease [16], Alzheimer's disease [17], frontotemporal lobar degeneration [18], B cell lymphoma [19], and especially depression [20].

The latest clinical research has shown significant increases in serum sortilin levels in MDD individuals compared with controls [21]. Preclinical research has shown that sortilin knockout mice are less likely to exhibit depressive-like behavior, and the underlying mechanism indicates that sortilin deficiency leads to the inhibition of TREK-1 expression and function, which strengthens dorsal raphe nucleus 5-hydroxytryptamine (5-HT) neuronal firing activity [22]. In another study, ablation of sortilin in mice did not alter their cognitive functions and depressive-like behavior; however, the mice exhibited anxiety-like behavior [23]. This evidence indicates that sortilin may participate in the pathological course of depression, although its precise role and molecular mechanism in depression remains to be determined.

Several studies have reported an association between sortilin and acid sphingomyelinase (ASM). Sortilin-deficient hepatocytes

[1]New Drug Screening Center, Jiangsu Center for Pharmacodynamics Research and Evaluation, China Pharmaceutical University, Nanjing 210009, China
Correspondence: Hong Liao (hliao@cpu.edu.cn)

Received: 9 July 2021 Accepted: 10 November 2021
Published online: 20 December 2021

appear to have lower ASM enzyme activity [23]. Sortilin in macrophages mediates ASM trafficking from the TGN to the lysosome [24]. These findings suggest that sortilin may mediate ASM trafficking within cells and is important for maintaining ASM enzyme activity. Therefore, whether sortilin contributes to depression pathogenesis by modulating ASM enzyme activity requires further exploration.

In the present study, we investigated the role of sortilin in the pathogenesis of depression. The results of this study will provide a novel potential target for MDD treatment.

MATERIALS AND METHODS

Animals

C57BL/6J male mice (7–8-week-old; Beijing Vital River Laboratory Animal Technology Co., Beijing, China) were used for all experiments. The mice were housed in cages and maintained in a standard animal room (12-h light/12-h dark cycles; 24 ± 2 °C; food and water ad libitum). The mice were acclimated to the new environment for 1 week before the start of all experiments. All procedures were performed in accordance with the guidelines of the Animal Research Ethics Committee of China Pharmaceutical University.

Chronic unpredictable mild stress (CUMS) procedure

The depression model was established using chronic unpredictable mild stress (CUMS) as previously described, with slight modifications [23]. Briefly, mice were individually housed and randomly exposed to the following stressors daily: cage shaking (1 time/s, 5 min); 45° cage tilting (8 h); tail pinching (2 min); tail pinching (5 min); warm water swim (37 ± 2 °C, 10 min); cold water swim (10 ± 2 °C, 5 min); moist bedding (24 h); empty cage without bedding (24 h); overnight illumination (12 h); restraining (4 h); food deprivation (24 h); water deprivation (24 h); no stress. Each individual stressor could not be repeated the next day. The procedure lasted 6 weeks.

Stereotactic surgeries

For stereotaxic delivery of AAV9-Sort1-shRNA (Hanbio Biotechnology Co. Ltd., Shanghai, China) or AAV9-Sort1 (Vigene Biosciences, Jinan, China), mice were anesthetized with isoflurane (2% induction, 1.5% maintenance) and affixed in a stereotaxic apparatus (RWD Life Science, Shenzhen, China). After exposing the skull, four small holes were made to allow bilateral microinjection (1 μL per side over 5 min) into the prefrontal cortex or hippocampus using a 1 μL Hamilton syringe. Coordinates were as follows: left and right prefrontal cortex (AP + 1.8 mm; ML ± 0.3 mm; DV − 2.0 mm from the bregma) or left and right hippocampus (AP − 2.3 mm; ML ± 1.8 mm; DV − 2.0 mm from the bregma). After every injection, the needle was left in place for an additional 5 min before withdrawal. Mice were left to recover for 4 weeks. Blank control adeno-associated virus vectors for AAV9-Sort1-shRNA and AAV9-Sort1 were injected in Ctrl AAV1 and Ctrl AAV2 group mice, respectively.

Drug administration

For ASM inhibitor (SR33557, MCE, 4 μg/μL) infusion in the prefrontal cortex and hippocampus, mice were anesthetized with isoflurane (2% induction, 1.5% maintenance) and affixed in a stereotaxic apparatus (RWD Life Science). After exposing the skull, mice were bilaterally microinjected (2.5 μL per side over 10 min) either with SR33557 or vehicle (10% DMSO + 90% corn oil) into the prefrontal cortex or hippocampus using a 10 μL Hamilton syringe. Coordinates were as follows: left and right prefrontal cortex (AP + 1.8 mm; ML ± 0.3 mm; DV − 2.0 mm from the bregma) or left and right hippocampus (AP − 2.3 mm; ML ± 1.8 mm; DV − 2.0 mm from the bregma). After every injection, the needle was left in place for an additional 5 min before withdrawal.

Behavioral tests

Open-field test (OFT). The open-field test (OFT) was performed as previously described [25]. Briefly, the mice were gently placed in the center of a cube chamber (45 cm × 45 cm × 45 cm) and left to explore the area for 6 min. An overhead camera recorded all behavior. The locomotor activity data including the trackpath, total distance traveled, and time spent in the center were analyzed using ANY-maze software (Stoelting Co., Wood Dale, IL, USA).

Tail suspension test (TST). The tail suspension test (TST) was performed as previously described [26]. Briefly, mice were individually tail-suspended with an adhesive tape that was placed 1 cm from the tip of the tail. The distance from the mouse head to the experiment table was 20 cm. Immobility time was measured manually during a 6-min test period.

Forced swimming test (FST). The forced swimming test (FST) was performed as previously described [27]. Briefly, mice were placed into a clear plastic cylinder (diameter 16 cm; height 30 cm) filled with 15 cm of water (23 ± 2 °C) for 6 min. Immobility time was measured manually during the last 4 min of the 6-min trial.

Novelty-suppressed feeding test (NSFT). The novelty-suppressed feeding test (NSFT) was performed as previously described [28]. Briefly, mice were deprived of food for 24 h before the test. Fresh mice chow covered with bedding was placed in the center of a cube chamber (45 cm × 45 cm × 45 cm) and the mouse was placed into the cube chamber for free activity for 5 min. The first time the mouse began eating the chow was recorded as latency to feed time.

Sucrose preference test (SPT). The sucrose preference test (SPT) was performed as previously described [29]. Briefly, mice were first habituated to drink from two bottles, one filled with water and the other with 1% sucrose solution, for 2 days, the side of the sucrose bottle being alternated each day. Then, after 24-h deprivation of water, the two bottles were presented again to allow mice to drink freely, and the water and 1% sucrose solution consumed over a 4-h period were measured. The sucrose preference index is defined as (sucrose consumed) / (sucrose consumed + water consumed) × 100 percentage index.

ASM activity measurement

Different brain regions were removed, flash-frozen, and lysed in 250 mM sodium acetate (pH 5.0), 1% NP40, and 1.3 mM EDTA for 15 min. The tissues were then homogenized using a tissue homogenizer at 1500 r/min and 30 s/cycle for four cycles at 4 °C. The homogenate was centrifuged at 12,000 r/min for 10 min at 4 °C. Aliquots of the supernatant were used for subsequent ASM activity measurement using the Fluorometric Acidic Sphingomyelinase Assay Kit (AAT Bioquest, Sunnyvale, CA, USA) following the manufacturer's instructions. Briefly, the testing samples were mixed with equal volumes of sphingomyelin working solution and incubated at 37 °C for 3 h. Then, we added equal volumes of sphingomyelinase working solution to each well and incubated the wells at room temperature for 1.5 h. Finally, the fluorescence intensity of each well was monitored using a fluorescence microplate reader at Ex/Em = 540/590 nm [30].

Total ceramide ELISA measurement

The different brain regions were removed, flash-frozen, and lysed in 0.01 M phosphate-buffered saline (PBS) (pH 7.4) for 10 min. The tissues were then homogenized using a tissue homogenizer at 1500 r/min, 30 s/cycle, 4 cycles, 4 °C. The homogenate was centrifuged at 3000 r/min, 20 min, 4 °C. Aliquots of the supernatant were used in subsequent total ceramide measurements using a mouse ceramide ELISA kit (Tongwei Co., Shanghai, China)

following the manufacturer's instructions. Briefly, the standards or samples were mixed with horseradish peroxidase-conjugate reagent and incubated at 37 °C for 60 min. The liquid was discarded and dried by swinging, and then washing buffer was added to the mixed solution to wash each well thoroughly. The solution was drained and the same washing procedure was repeated five times. Each well was patted dry, and chromogen solution A and chromogen solution B were added to each well; the wells were then left in the dark at 37 °C for 15 min. Finally, the stop solution was added and the absorbance of each well was read at 450 nm within 15 min.

Tissue preparation

Mice were anesthetized with isoflurane and perfused with 0.9% saline followed by cold 4% paraformaldehyde. The whole brain tissues were fixed in 4% paraformaldehyde at 4 °C overnight and then dehydrated in a gradient of 20% sucrose and 30% sucrose at 4 °C. When the brain tissues were fully dehydrated, they were sliced on a Leica1950 cryostat (Leica Instruments, Wetzlar, Germany) into 12-μm sections and stored at −20 °C for immunofluorescence staining.

Immunofluorescence staining

Brain sections were permeabilized with 0.3% Triton X-100 in PBS, blocked with 10% goat serum in 90% PBS at room temperature for 1 h, and then incubated with primary antibody at 4 °C overnight. The following primary antibodies were used: goat anti-Sortilin (1:200, R&D Systems, Inc., Minneapolis, MN, USA); rabbit anti-NeuN (1:300, Abcam, Cambridge, MA, USA); rabbit anti-ASM (1:200, Abcam); mouse anti-TGN38 (1:100, R&D); mouse anti-LAMP1 (1:100, R&D). After the sections were rinsed with PBS three times, they were incubated with Alexa Fluor 488 conjugated donkey anti-goat IgG (1:500, Invitrogen, Waltham, MA, USA), Alexa Fluor 633 conjugated donkey anti-rabbit IgG (1:500, Invitrogen), Alexa Fluor 633 conjugated donkey anti-mouse IgG (1:500, Invitrogen), Alexa Fluor 488 conjugated goat anti-rabbit IgG (1:500, Invitrogen), or Alexa Fluor 633 conjugated goat anti-mouse IgG (1:500, Invitrogen) at room temperature for 1 h with Hoechst 33342 (1:1,000, Invitrogen). The images were captured using an Olympus FV1000 confocal microscope and processed with Image J software.

Western blot analysis

Different brain regions were lysed in radio immunoprecipitation assay lysate (Beyotime, Haimen, China) with complete protease inhibitor cocktail added (Roche, Indianapolis, IN, USA). Equal amounts of protein were separated on SDS polyacrylamide gels, transferred to polyvinyl-difluoride membranes (Millipore, Burlington, MA, USA), and blocked with 3% (w/v) bovine serum albumin. The membranes were incubated with the following primary antibodies: goat anti-sortilin (1:500, R&D); mouse anti-PSD95 (1:1,000, CST, Danvers, MA, USA); mouse anti-SYP38 (1:1,000, Abcam); rabbit anti-ROCK2 (1:500, ABclonal, Wuhan, China); rabbit anti-p-cofilin (1:500, CST); rabbit anti-cofilin (1:1,000, CST); rabbit anti-ASM (1:500, Abcam); mouse anti-β-actin (1:2,000, Santa Cruz Biotechnology, Santa Cruz, CA, USA); mouse anti-GAPDH (1:2,000, Sino Biological, Beijing, China), at 4 °C overnight. After rinsing in Tris-buffered saline and Tween 20 (TBST) three times, the membranes were incubated with the corresponding secondary antibody at room temperature for 1 h. After rinsing with TBST four times, the labeled proteins were detected using the Bio-Rad System (Bio-Rad, Feldkirchen, Germany).

RhoA activity measurement

Activated RhoA was determined using the RhoA Pulldown Activation Assay Kit (#BK036, Cytoskeleton Inc., Denver, CO, USA). Briefly, different brain regions were homogenized using a pellet pestle in 10 mg tissue/200 μL lysis buffer. Homogenates were centrifuged and supernatants were incubated with Rhotekin-RBD Beads to pull down active RhoA. After appropriate processing, the samples were analyzed using Western blot.

Golgi staining

Golgi staining was performed using the FD Rapid GolgiStain Kit (FD NeuroTechnologies, Inc., Columbia, MD, USA), following the manufacturer's instructions. Mice were anesthetized with isoflurane and the whole brains were quickly removed and rinsed with double-distilled water. After removing the olfactory bulb and cerebellum with a blade, the brain tissues were immersed in Golgi impregnation solution (solutions A and B) overnight and then stored in fresh solution for 2 weeks in the dark at room temperature. Brains were transferred into solution C overnight and then stored in fresh solution for 3 days in the dark at room temperature. The brain tissues were sliced into 100-μm-thick sections on a Leica1950 cryostat (Leica Instruments) and each section was mounted in solution C on a gelatin-coated microscope slide. When the sections had dried naturally, the staining procedure was performed following the manufacturer's instructions. Images of dendritic spines within the prefrontal cortex and hippocampus were captured using a 100× oil objective lens using an Olympus FV1000 confocal microscope [31, 32].

Statistical analysis

Data were presented as mean ± standard error of the mean (SEM) with individual data points overlaid. All statistical tests were performed in GraphPad Prism 6.0 (La Jolla, CA, USA). Individual comparisons were assessed using an two-sided Student's *t*-test and multiple comparisons were performed using one-way analysis or two-way analysis of variance with Holm–Sidak's *post hoc* tests or Bonferroni's *post hoc* tests. All tests were considered statistically significant at $P < 0.05$.

RESULTS

Increased sortilin expression and ASM/ceramide levels in the prefrontal cortex and hippocampus in mice exposed to CUMS

To explore whether sortilin is involved in the pathogenesis of depression, the CUMS model, a classical rodent model of depression, was used in this study. After performing CUMS, the CUMS mice showed significant loss in body weight, less time spent in the central zone in the OFT, more immobility time in the TST and FST, and less sucrose preference in the SPT (Supplementary Fig. S1a–e). These results showed the CUMS was successful in inducing depressive-like behaviors in the mice. Then, the sortilin protein expression in the four brain regions highly relevant for depression (prefrontal cortex, hippocampus, nucleus accumbens, and amygdala) was examined. Western blot analysis showed that sortilin protein expression increased in the prefrontal cortex and hippocampus of CUMS mice ($F_{3,40} = 11.54$, $P < 0.0001$; Fig. 1a, b); however, statistical differences were not observed in the nucleus accumbens and amygdala of CUMS mice compared with stress-naive mice (Fig. 1a, b). Subsequent immunofluorescence staining results verified further that sortilin was highly expressed in the two brain regions of CUMS mice ($F_{1,14} = 37.77$, $P < 0.0001$; Fig. 1c–e).

Because ASM/ceramide abnormality is highly associated with depression [33–36], ASM enzyme activity was tested using a Fluorometric Acidic Sphingomyelinase Assay Kit and total ceramide levels were tested using a ceramide ELISA kit separately in the four brain regions mentioned above. The results showed upregulated ASM enzyme activity in the prefrontal cortex and hippocampus of CUMS mice ($F_{1,16} = 47.17$, $P < 0.0001$), and upregulated total ceramide levels were observed in the prefrontal cortex, hippocampus, and nucleus accumbens of CUMS mice ($F_{1,24} = 67.53$, $P < 0.0001$; Fig. 1f, g). Overall, these results indicated that sortilin and ASM/ceramide levels were significantly increased in the prefrontal cortex and hippocampus of mice exposed to CUMS. The coincident upregulation of sortilin and ASM/ceramide

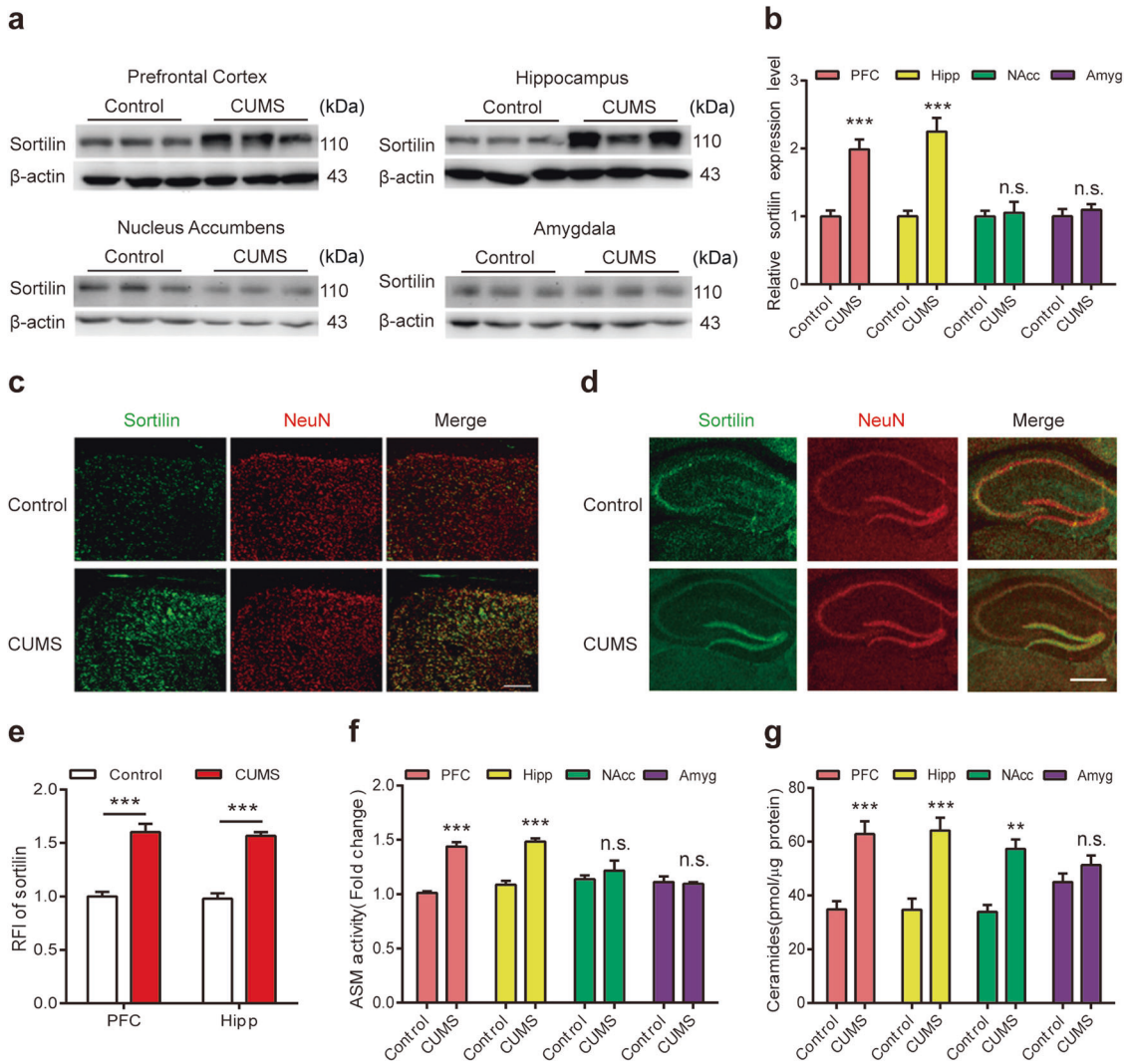

Fig. 1 Increased sortilin expression and ASM/ceramide levels in the prefrontal cortex and hippocampus in mice exposed to CUMS. **a**, **b** Western blot analysis of sortilin protein expression in the prefrontal cortex (PFC), hippocampus (Hipp), nucleus accumbens (NAcc), amygdala (Amyg) of mice. $n = 4$–5 per group. ***$P < 0.001$ compared with control. **c**, **d** Representative images of immunostaining for sortilin in the PFC (**c**) and Hipp (**d**) of mice. Scale bars = 200 μm. **e** Quantitative of relative fluorescence intensity (RFI) in the PFC and Hipp of mice. $n = 3$–4 per group. ***$P < 0.001$ compared with control. **f**, **g** Levels of acid sphingomyelinase (ASM) activity (**f**) and quantitative ELISA analysis of total ceramide (**g**) in the PFC, Hipp, NAcc, Amyg of mice. $n = 3$–4 per group. **$P < 0.01$, ***$P < 0.001$ compared with control. One-way ANOVA, Holm–Sidak's multiple comparisons test. All data are represented as mean ± SEM.

levels indicates that sortilin and ASM/ceramide signaling may be involved in the pathogenesis of depression.

Specific knockdown of sortilin in the prefrontal cortex and hippocampus of mice ameliorates CUMS-induced depressive-like behaviors

To examine the potential role of sortilin in depression, AAV9-Sort1-shRNA or AAV9-Ctrl was stereotaxically injected into the prefrontal cortex and hippocampus to construct specific sortilin knockdown mice. AAV9-Sort1-shRNA was confirmed to reduce sortilin protein expression effectively in the prefrontal cortex and hippocampus (Supplementary Fig. S2a, b). After achieving specific knockdown of sortilin, these mice were subjected to CUMS. After completing CUMS, a series of tests were performed to detect depressive-like behaviors. In the OFT, sortilin knockdown mice did not show significant differences in total distance traveled compared with AAV9-Ctrl-injected mice in the CUMS and stress-naive models ($F_{1,31} = 0.02072$, $P = 0.8865$; Fig. 2b). However, sortilin knockdown mice showed less immobility time ($F_{1,29} = 5.238$, $P = 0.0296$) and significantly increased time spent in the central zone than did AAV9-Ctrl-injected mice in the CUMS model but not in the stress-naive model ($F_{1,34} = 3.711$, $P = 0.0625$; Fig. 2b). The sortilin knockdown mice showed no significant difference in body weight gain compared with AAV9-Ctrl-injected mice in the CUMS and stress-naive models, although sortilin knockdown mice showed a minimally increased trend in body weight gain compared with AAV9-Ctrl-injected mice in the CUMS model ($F_{1,36} = 1.527$, $P = 0.2245$; Fig. 2a). Sortilin knockdown mice exhibited reduced immobility time compared with AAV9-Ctrl-injected mice in the CUMS model but not in the stress-naive model in the TST ($F_{1,36} = 5.741$, $P = 0.0219$; Fig. 2c) and in the FST ($F_{1,34} = 8.794$, $P = 0.0055$; Fig. 2d). In accordance with the above results, latency to feed time was less in sortilin knockdown mice than in AAV9-Ctrl-injected mice in the CUMS model but not in the stress-naive model ($F_{1,35} = 2.6$, $P = 0.1159$; Fig. 2e). In addition, sortilin knockdown mice showed greater preference for sucrose water than AAV9-Ctrl-injected mice after CUMS, however, the stress-naive mice did not show a preference ($F_{1,42} = 10.11$, $P = 0.0028$; Fig. 2f). Collectively,

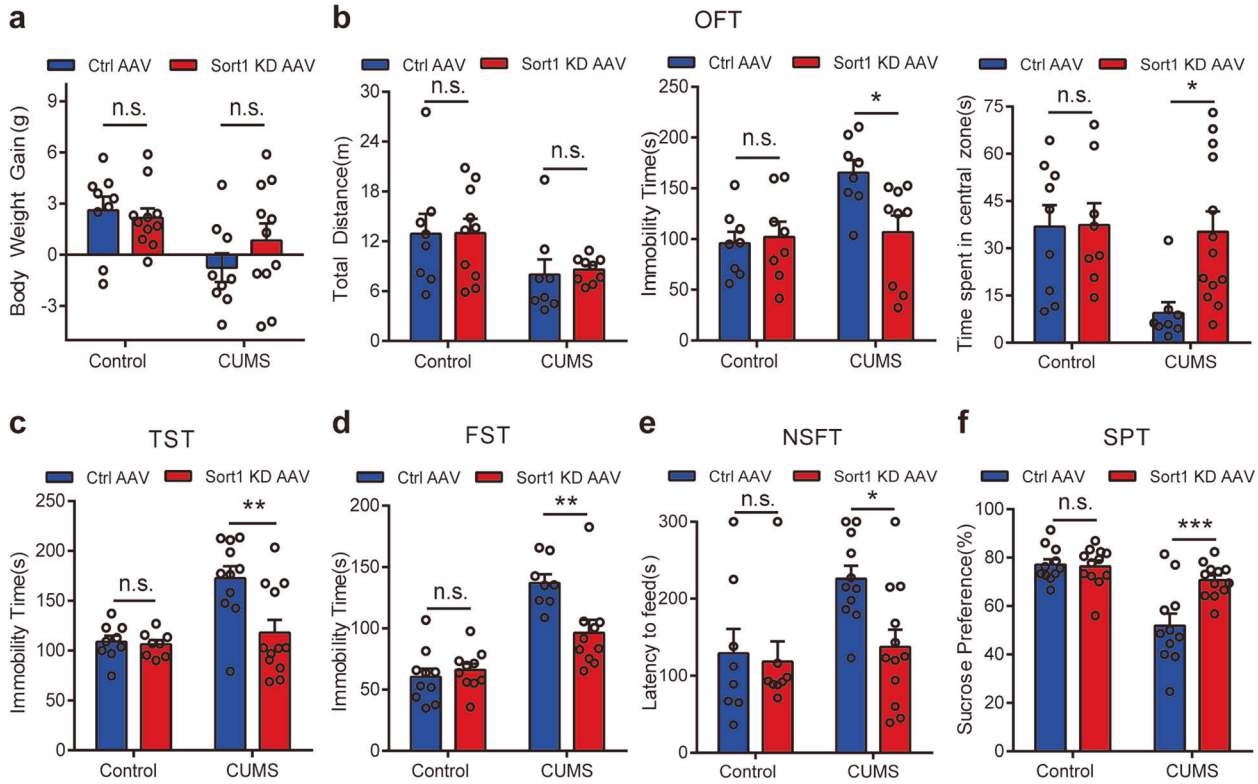

Fig. 2 Specific knockdown of sortilin in the prefrontal cortex and hippocampus of mice ameliorates CUMS-induced depressive-like behaviors. **a** Body weight changes from the beginning to the end of the experiment in the mice. $n = 8$–16 per group. **b** Total distance, immobility time, time spent in central zone in the OFT. $n = 8$–16 per group. **c** Immobility time in the TST. $n = 8$–16 per group. **d** Immobility time in the FST. **e** Latency to feed time in the NSFT. $n = 8$–16 per group. **f** Percentage of sucrose preference in the SPT. $n = 8$–16 per group. $^{*}P < 0.05$, $^{**}P < 0.01$, $^{***}P < 0.001$ compared with CUMS + Ctrl AAV. One-way ANOVA, Holm–Sidak's multiple comparisons test. All data are represented as mean ± SEM.

these results demonstrated that specific knockdown of sortilin in the prefrontal cortex and hippocampus ameliorates depressive-like behaviors under the CUMS condition. However, when mice were not subjected to CUMS, sortilin knockdown mice and AAV9-Ctrl-injected mice did not show significant differences in any depressive-like behavior test.

ASM distribution between the TGN and lysosome regulated by sortilin affects ASM/ceramide levels

In previous studies, sortilin was shown to mediate ASM trafficking from the TGN to the lysosome in several types of cells [24, 37]. In the present study, the effects of sortilin knockdown on ASM transport and ASM/ceramide levels in the prefrontal cortex and hippocampus were examined. Using the Fluorometric Acidic Sphingomyelinase Assay Kit, sortilin knockdown mice had lower ASM enzyme activity than AAV9-Ctrl-injected mice in the prefrontal cortex ($F_{1,8} = 156.8$, $P < 0.0001$) and hippocampus ($F_{1,8} = 40.45$, $P = 0.0002$) in the CUMS and stress-naive models (Fig. 3a). Next, the ceramide levels were examined using a mouse ceramide ELISA kit. The results also showed sortilin knockdown mice had lower total ceramide levels than AAV9-Ctrl-injected mice in the prefrontal cortex ($F_{1,8} = 107.1$, $P < 0.0001$) and hippocampus ($F_{1,8} = 114.3$, $P < 0.0001$) in the CUMS and stress-naive models (Fig. 3b), which exhibited a trend similar to the ASM enzyme activity outcome. These results proved, preliminarily, that sortilin plays a critical role in regulating ASM/ceramide signaling.

To determine the mechanism by which sortilin regulates ASM/ceramide signaling, an immunofluorescence co-localization technique was used to detect ASM distribution between the TGN and the lysosome. In the prefrontal cortex of stress-naive mice, knockdown of sortilin increased ASM and TGN38 (TGN marker) co-localization levels ($F_{1,13} = 24.44$, $P = 0.0003$; Fig. 3c, g) but decreased ASM and LAMP1 (lysosome marker) co-localization levels ($F_{1,15} = 31.51$, $P < 0.0001$; Fig. 3d, h). Furthermore, in the CUMS model, knockdown of sortilin increased ASM and TGN38 co-localization levels ($F_{1,13} = 24.44$, $P = 0.0003$; Fig. 3c, g) but decreased ASM and LAMP1 co-localization levels ($F_{1,15} = 31.51$, $P < 0.0001$; Fig. 3d, h). These results confirmed knockdown of sortilin hindered ASM trafficking from the TGN to the lysosome under normal and CUMS conditions. In addition, the CUMS paradigm decreased ASM and TGN38 co-localization levels ($F_{1,13} = 20.54$, $P = 0.0006$; Fig. 3c, g) and increased ASM and LAMP1 co-localization levels ($F_{1,15} = 13.83$, $P = 0.0021$; Fig. 3d, h), indicating CUMS facilitated ASM trafficking from the TGN to the lysosome. The representative hippocampus pictures showed similar outcomes with the prefrontal cortex (Fig. 3e, f, i, j). Taken together, our data demonstrated that sortilin facilitates ASM trafficking from the TGN to the lysosome, which promotes ASM maturation in the lysosome, ultimately leading to upregulation of ASM enzyme activity and total ceramide levels.

Sortilin overexpression induces depressive-like behaviors by promoting ASM/ceramide levels

To verify the role of sortilin in depression, AAV9-Sort1 was injected into the prefrontal cortex and hippocampus to construct specific sortilin overexpression mice and sortilin was confirmed to be overexpressed in the two brain regions (Supplementary Fig. S2c, d). The body weight gain was not significantly different between AAV9-Sort1-injected mice and AAV9-Ctrl-injected mice ($P = 0.6733$; Fig. 4a). Next, the depressive-like behaviors in AAV9-Sort1-injected mice and AAV9-Ctrl-injected mice were compared. The AAV9-Sort1-injected mice did not show any

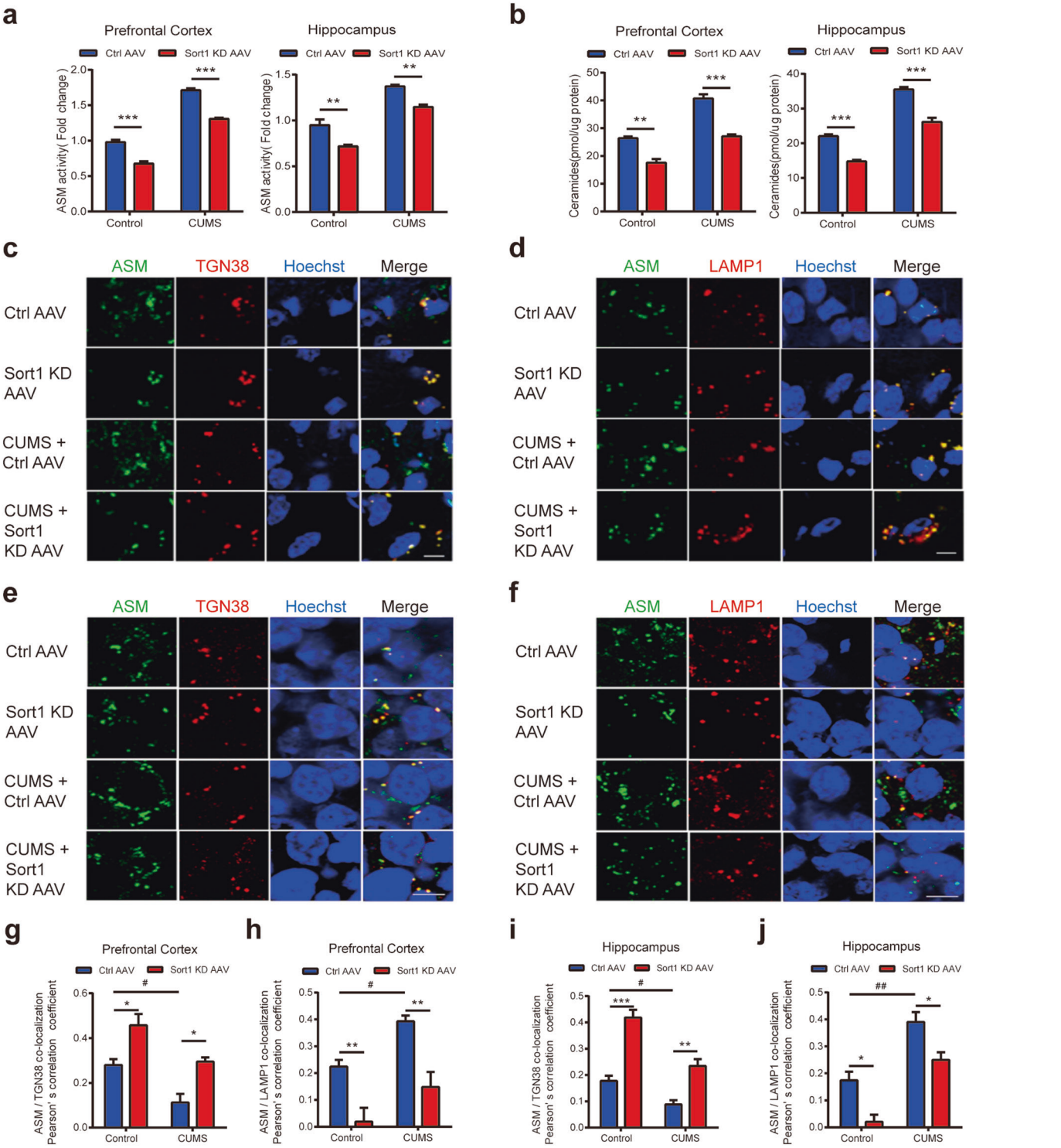

Fig. 3 ASM distribution between the TGN and lysosome regulated by sortilin affects ASM/ceramide levels. a, **b** Levels of ASM activity (**a**) and quantitative ELISA analysis of total ceramide (**b**) in the PFC and Hipp of mice. $n = 5$ per group. **c**, **d** Representative images of immunostaining for ASM, TGN38, Hoechst (**c**) and ASM, LAMP1, Hoechst (**d**) in the PFC of mice. **e**, **f** Representative images of immunostaining for ASM, TGN38, Hoechst (**e**) and ASM, LAMP1, Hoechst (**f**) in the Hipp of mice. Scale bars = 5 μm. **g**, **h** Quantitative of ASM/TGN38 (**g**) and ASM/LAMP1 (**h**) co-localization Pearson's correlation coefficient in the PFC of mice. $n = 3$–4 per group. **i**, **j** Quantitative of ASM/TGN38 (**i**) and ASM/LAMP1 (**j**) co-localization Pearson's correlation coefficient in the Hipp of mice. $n = 3$–4 per group. $^{\#}P < 0.05$, $^{\#\#}P < 0.01$ compared with Ctrl AAV; $^{*}P < 0.05$, $^{**}P < 0.01$, $^{***}P < 0.001$ compared with Ctrl AAV or CUMS + Ctrl AAV. One-way ANOVA, Holm–Sidak's multiple comparisons test. All data are represented as mean ± SEM.

change in total distance traveled ($P = 0.8068$), immobility time ($P = 0.8283$), or time spent in the central zone ($P = 0.2313$) compared with AAV9-Ctrl-injected mice (Fig. 4b). The AAV9-Sort1-injected mice displayed longer immobility time compared with AAV9-Ctrl-injected mice in the TST ($P < 0.0001$; Fig. 4c) and FST ($P = 0.0003$; Fig. 4d). Consistent with the above results, AAV9-Sort1-injected mice also showed increased latency to feed time compared with AAV9-Ctrl-injected mice in the NSFT ($P = 0.0065$; Fig. 4e). Anhedonia, the core symptom of depression, was tested using the SPT. The AAV9-Sort1-injected mice drank less sucrose water than AAV9-Ctrl-injected mice ($P < 0.0001$; Fig. 4f). These results confirmed that sortilin overexpression in the prefrontal cortex and hippocampus is sufficient to induce depressive-like behaviors in stress-naive mice.

To investigate how specific sortilin overexpression affects depressive-like behaviors, the changes in ASM/ceramide levels were examined. ASM enzyme activity was upregulated in the prefrontal cortex ($P = 0.0003$) and hippocampus ($P = 0.0232$) in AAV9-Sort1-injected mice (Fig. 4g). Total ceramide levels was upregulated in the prefrontal cortex ($P = 0.0093$) and hippocampus ($P = 0.0416$) in AAV9-Sort1-injected mice (Fig. 4h), which was consistent with the ASM enzyme activity results. Then, using the immunofluorescence co-localization technique, the effects of sortilin overexpression on distribution of ASM in the TGN and lysosome were determined. In the prefrontal cortex, sortilin overexpression decreased ASM and TGN38 co-localization levels ($P = 0.0443$; Fig. 4i, m) and simultaneously increased ASM and LAMP1 co-localization levels ($P = 0.0144$; Fig. 4j, n). Similar results were observed in the hippocampus, indicating that sortilin overexpression promoted the transport of ASM from the TGN to the lysosome ($P = 0.0057$ for ASM and TGN38 co-localization, $P = 0.0223$ for ASM and LAMP1 co-localization; Fig. 4k, l, o, p). In addition, total ASM protein levels in the prefrontal cortex and hippocampus of AAV9-Sort1-injected mice did not change compared with AAV9-Ctrl-injected mice (Supplementary Fig. S4a, b). These data indicated that the mechanism of specific sortilin overexpression in the prefrontal cortex and hippocampus induced depressive-like behaviors. Excessive sortilin promoted ASM trafficking from the TGN to the lysosome and led to the enrichment of activated ASM in lysosomes, which hydrolyzed sphingomyelin to ceramide, finally resulting in ceramide upregulation in the two brain regions.

Sortilin regulates dendritic spine dynamics

The above results indicated that sortilin-regulated ASM/ceramide signaling influences depressive-like behaviors. The potential mechanism of how ASM/ceramide signaling affects depressed mood remains to be clarified. In a previous study, the abnormality of dendritic spines was shown to be highly associated with depression. In the present study, the influence of specific sortilin knockdown on dendritic spine number and morphology was investigated. Based on Golgi staining, sortilin knockdown restored the loss of dendritic spines caused by CUMS in the prefrontal cortex ($F_{1,12} = 22.99$, $P = 0.0004$; Fig. 5a) and hippocampus ($F_{1,12} = 26.35$, $P = 0.0002$; Fig. 5b) but did not affect dendritic spine number of mice not exposed to CUMS (Fig. 5a, b). Analysis of dendritic spine dynamics showed that sortilin knockdown reversed the reduction of mushroom spines and the increase of thin spines caused by CUMS in the prefrontal cortex and hippocampus but did not influence stubby spines (Fig. 5a, b).

Next, the effects of sortilin knockdown on the expression of synapse-associated proteins were investigated. SYP38 is a presynaptic-related protein and PSD95 a postsynaptic-related protein. Western blot analysis showed that CUMS could induce the downregulation of SYP38 and PSD95, which is consistent with previous research (Fig. 5c, d). After CUMS, sortilin knockdown mice had increased SYP38 and PSD95 expression in the prefrontal cortex ($F_{1,12} = 39.83$, $P < 0.0001$ and $F_{1,12} = 20.65$, $P = 0.0007$, respectively; Fig. 5c) and hippocampus ($F_{1,12} = 12.21$, $P = 0.0044$ and $F_{1,12} = 20.12$, $P = 0.0007$, respectively; Fig. 5d) compared with AAV9-Ctrl-injected mice. However, knockdown of sortilin in the prefrontal cortex and hippocampus did not affect the SYP38 and PSD95 expression in stress-naive mice (Fig. 5c, d). In addition, AAV9-Sort1-injected mice had lower SYP38 and PSD95 expression than AAV9-Ctrl-injected mice in the prefrontal cortex ($P = 0.0124$ and $P = 0.0022$, respectively; Fig. 5e) and hippocampus ($P = 0.001$ and $P = 0.0088$, respectively; Fig. 5f). The results demonstrated that sortilin regulates depressive-like behaviors by affecting dendritic spines, although the specific signaling pathway in this process remains unknown.

Sortilin plays a regulatory role in RhoA/ROCK2 signaling

In previous studies, RhoA/ROCK signaling was shown to play an important role in the regulation of dendritic spine dynamics in depressive disorders [38–40]. In the present study, we investigated the influence of sortilin on the RhoA/ROCK signaling pathway. RhoA Pulldown Activation Assay Kit and subsequent Western blot analysis results showed that CUMS increased the activation of RhoA, and specific sortilin knockdown reversed this increase in the prefrontal cortex ($F_{5,18} = 5.532$, $P = 0.0029$; Fig. 6a). However, specific sortilin knockdown did not affect RhoA activation in the prefrontal cortex of stress-naive mice (Fig. 6a). In addition, specific sortilin overexpression was sufficient to cause enhanced RhoA activation in the prefrontal cortex (Fig. 6a), and similar results were obtained in the hippocampus ($F_{5,18} = 6.943$, $P = 0.0009$; Fig. 6b). In the CNS, ROCK2 is the main form of the ROCK family and is often activated simultaneously by RhoA [41]. Western blot analysis showed that the pattern of changes in ROCK2 activation was similar to those of activated RhoA in the prefrontal cortex ($F_{5,24} = 5.492$, $P = 0.0017$; Fig. 6c) and hippocampus ($F_{5,18} = 4.679$, $P = 0.0065$; Fig. 6d). Next, we investigated changes in the phosphorylation levels of cofilin, a key downstream signaling molecule that plays a critical role in dendritic spine dynamics. Western blot analysis showed that CUMS decreased cofilin phosphorylation; sortilin knockdown partially reversed this decrease in the prefrontal cortex of mice, except stress-naive mice ($F_{5,18} = 17.06$, $P < 0.0001$; Fig. 6e). Sortilin overexpression also led to the downregulation of cofilin phosphorylation in the prefrontal cortex (Fig. 6e); similar results were obtained in the hippocampus ($F_{5,18} = 8.936$, $P = 0.0002$; Fig. 6f). Collectively, these results demonstrate that sortilin regulates dendritic spine dynamics via RhoA/ROCK2 signaling in the prefrontal cortex and hippocampus.

ASM inhibitor reverses depressive-like behaviors induced by sortilin overexpression

To further examine whether ASM/ceramide signaling is the main pathway through which sortilin regulates depression, an ASM inhibitor, SR33557, was injected into the prefrontal cortex and hippocampus of mice to inhibit ASM enzyme activity. ASM enzyme activity test and total ceramide ELISA results confirmed that SR33557 (4 μg/μL) effectively reduced ASM/ceramide levels triggered by specific sortilin overexpression in the prefrontal cortex and hippocampus (Supplementary Fig. S5a, b). In the OFT, AAV9-Sort1+SR33557-injected mice did not show any change in total distance traveled ($P = 0.1112$), immobility time ($P = 0.3786$), or time spent in the central zone ($P = 0.9145$) compared with AAV9-Sort1+Solvent-injected mice (Fig. 7b). The body weight gain was not significantly different between the two groups ($P = 0.2123$; Fig. 7a). In the TST, SR33557 reversed the increase of immobility time induced by sortilin overexpression ($F_{2,45} = 39.3$, $P < 0.0001$; Fig. 7c). In the FST, SR33557 similarly reversed the increase of immobility time induced by sortilin overexpression ($F_{2,45} = 7.568$, $P = 0.0015$; Fig. 7d). In the NSFT, SR33557 significantly reversed the increased latency to feed time induced by sortilin overexpression ($F_{2,45} = 15.98$, $P < 0.0001$; Fig. 7e). In the SPT, SR33557 ameliorated the decrease of sucrose water intake

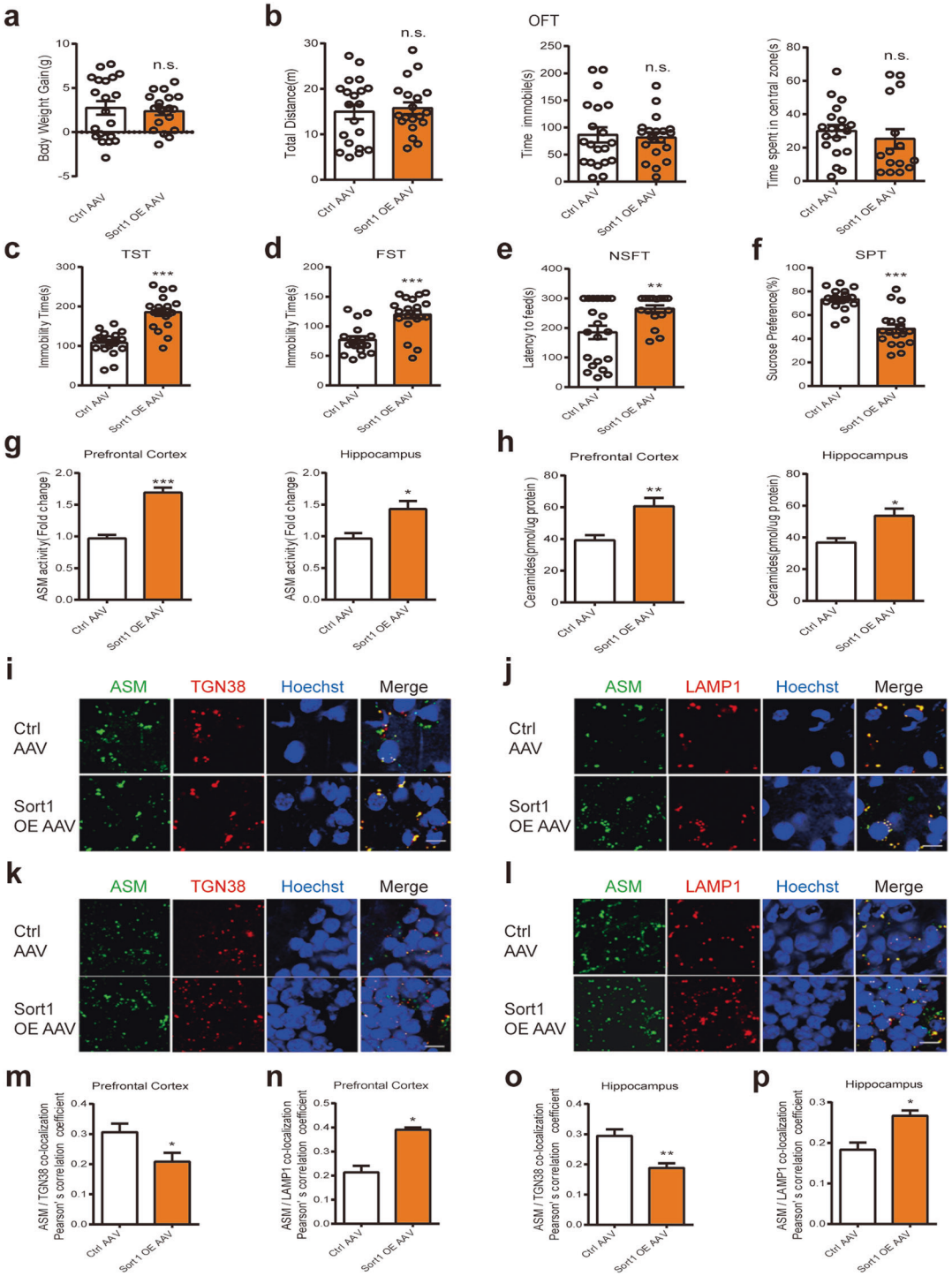

Fig. 4 Sortilin overexpression induces depressive-like behaviors by promoting ASM/ceramide levels. a Body weight gain of the mice. $n =$ 15–20 per group. **b** Total distance, immobility time, time spent in central zone in the OFT. $n = 10$–14 per group. **c** Immobility time in the TST. $n = 15$–20 per group. **d** Immobility time in the FST. $n = 15$–20 per group. **e** Latency to feed time in the NSFT. $n = 15$–20 per group. **f** Percentage of sucrose preference in the SPT. $n = 15$–20 per group. **g**, **h** Levels of ASM activity (**g**) and quantitative ELISA analysis of total ceramide (**h**) in the PFC and Hipp of mice. $n = 4$–5 per group. **i**, **j** Representative images of immunostaining for ASM, TGN38, Hoechst (**i**) and ASM, LAMP1, Hoechst (**j**) in the PFC of mice. **k**, **l** Representative images of immunostaining for ASM, TGN38, Hoechst (**k**) and ASM, LAMP1, Hoechst (**l**) in the Hipp of mice. Scale bars = 10 μm. **m**, **n** Quantitation of ASM/TGN38 (**m**) and ASM/LAMP1 (**n**) co-localization Pearson's correlation coefficient in the PFC of mice. $n = 5$ per group. **o**, **p** Quantitative of ASM/TGN38 (**o**) and ASM/LAMP1 (**p**) co-localization Pearson's correlation coefficient in the Hipp of mice. $n = 5$ per group. $^*P < 0.05$, $^{**}P < 0.01$, $^{***}P < 0.001$ compared with Ctrl AAV. Two-sided Student's *t*-test. All data are represented as mean ± SEM.

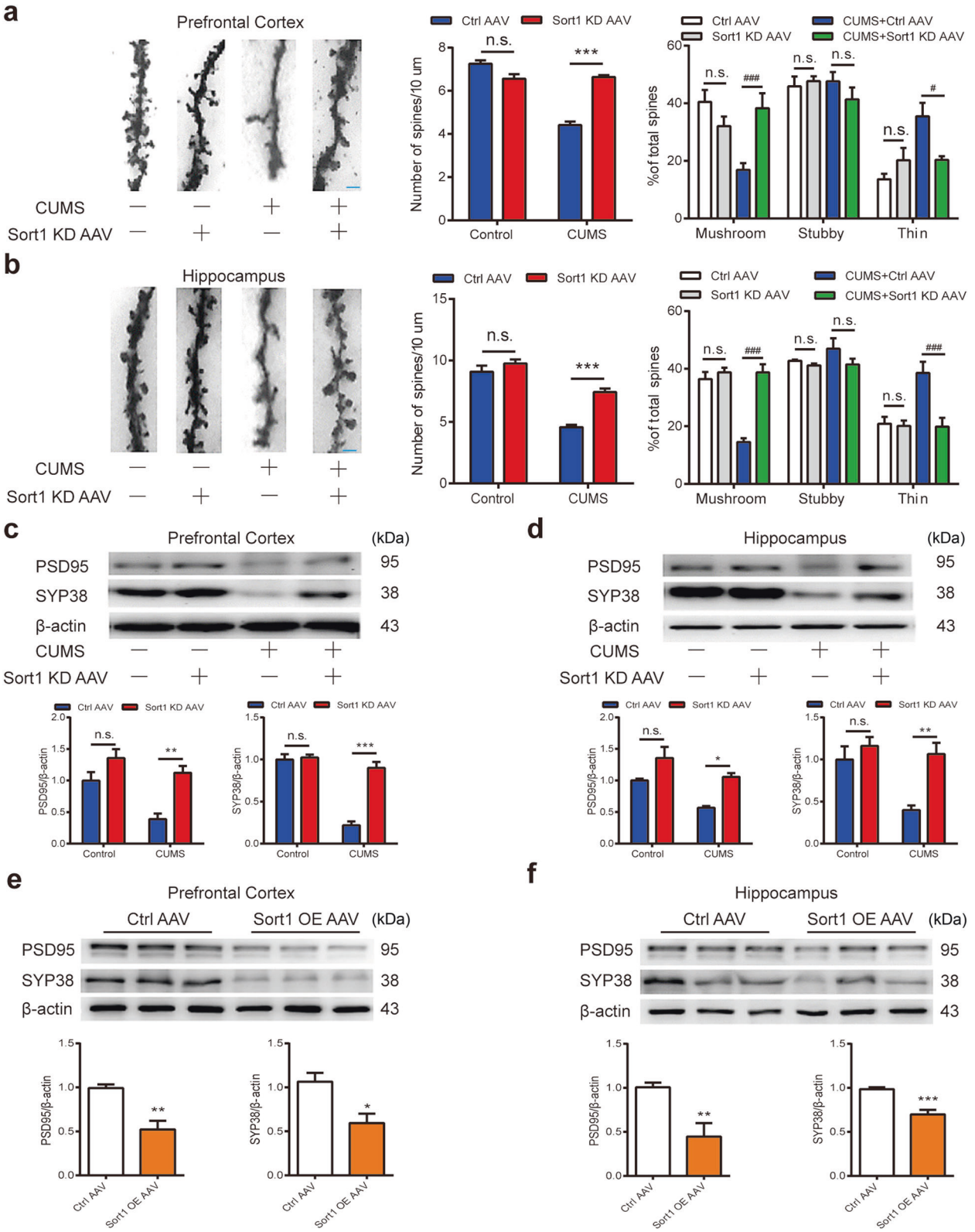

Fig. 5 Sortilin regulates dendritic spine dynamics. a, **b** Representative images of Golgi staining for dendritic spine and quantitative analysis of dendritic spine dynamics in the PFC (**a**) and Hipp (**b**) of mice. $n = 4$ per group. Scale bars = 2 μm. $^{***}P < 0.001$ compared with Ctrl AAV or CUMS + Ctrl AAV; $^{\#}P < 0.05$, $^{\#\#\#}P < 0.001$ compared with CUMS + Ctrl AAV. One-way ANOVA, Holm–Sidak's multiple comparisons test. **c**, **d** Western blot analysis of SYP38 and PSD95 expression in the PFC (**c**) and Hipp (**d**) of Sort1 KD mice. $n = 3$–5 per group. $^{*}P < 0.05$, $^{**}P < 0.01$, $^{***}P < 0.001$ compared with Ctrl AAV or CUMS + Ctrl AAV. One-way ANOVA, Holm–Sidak's multiple comparisons test. **e**, **f** Western blot analysis of SYP38 and PSD95 expression in the PFC (**e**) and Hipp (**f**) of Sort1 OE mice. $n = 4$–6 per group. $^{*}P < 0.05$, $^{**}P < 0.01$, $^{***}P < 0.001$ compared with Ctrl AAV. Two-sided Student's *t*-test. All data are represented as mean ± SEM.

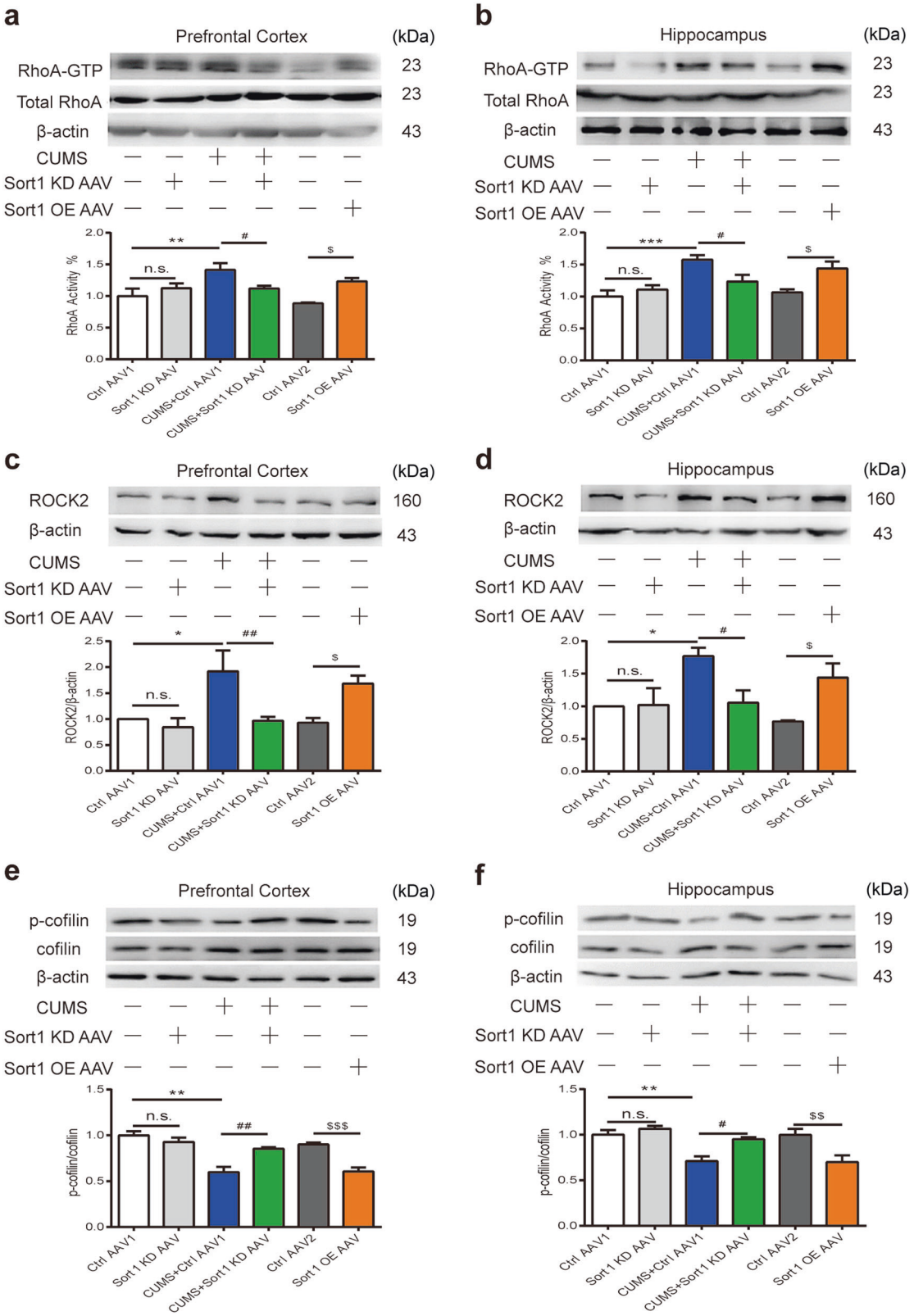

Fig. 6 Sortilin plays a regulatory role in RhoA/ROCK2 signaling. a, **b** RhoA activity test in the PFC (**a**) and Hipp (**b**) of mice. $n = 4$ per group. **c**, **d** Western blot analysis of ROCK2 protein expression in the PFC (**c**) and Hipp (**d**) of mice. $n = 4$–5 per group. **e**, **f** Western blot analysis of phosphorylation levels of cofilin in the PFC (**e**) and Hipp (**f**) of mice. $n = 3$–4 per group. $^{*}P < 0.05$, $^{**}P < 0.01$, $^{***}P < 0.001$ compared with Ctrl AAV1; $^{\#}P < 0.05$, $^{\#\#}P < 0.01$ compared with CUMS + Ctrl AAV1; $^{\$}P < 0.05$, $^{\$\$}P < 0.01$, $^{\$\$\$}P < 0.001$ compared with Ctrl AAV2. One-way ANOVA, Holm–Sidak's multiple comparisons test. All data are represented as mean ± SEM.

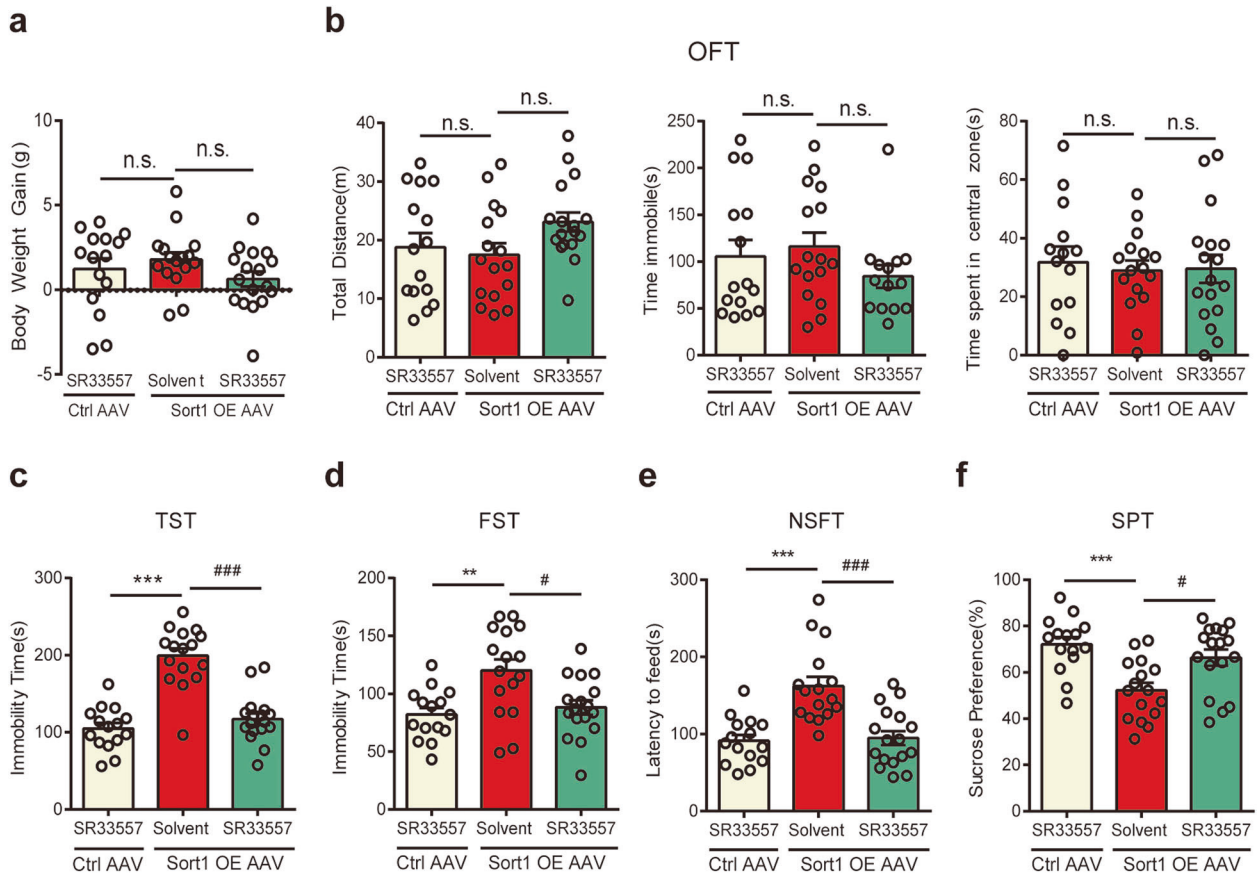

Fig. 7 ASM inhibitor reverses depressive-like behaviors induced by sortilin overexpression. a Body weight gain of the mice. $n = 15–17$ per group. **b** Total distance, immobility time, time spent in central zone in the OFT. $n = 14–17$ per group. **c** Immobility time in the TST. $n = 15–17$ per group. **d** Immobility time in the FST. $n = 15–17$ per group. **e** Latency to feed time in the NSFT. $n = 15–17$ per group. **f** Percentage of sucrose preference in the SPT. $n = 15–17$ per group. $^{**}P < 0.01$, $^{***}P < 0.001$ compared with Ctrl AAV + SR33557; $^{\#}P < 0.05$, $^{\#\#\#}P < 0.001$ compared with Sort1 OE AAV + Solvent. One-way ANOVA, Holm–Sidak's multiple comparisons test. All data are represented as mean ± SEM.

caused by sortilin overexpression ($F_{2,45} = 9.519$, $P = 0.0004$; Fig. 7f). These behavioral test results demonstrated that the inhibition of ASM enzyme activity can effectively reverse depressive-like behaviors resulting from specific sortilin overexpression in the prefrontal cortex and hippocampus.

Repression of ASM reverses loss of dendritic spines induced by sortilin overexpression

The above results show that ASM/ceramide signaling plays an important role in the regulation of sortilin in dendritic spine dynamics. Therefore, the influence of ASM inhibitor on dendritic spine dynamics and RhoA/ROCK2 signaling pathway in sortilin-overexpressed mice was investigated. Based on the Golgi staining experiment, SR33557 ameliorated dendritic spine loss induced by sortilin overexpression in the prefrontal cortex ($F_{2,9} = 66.43$, $P < 0.0001$) and hippocampus ($F_{2,9} = 20.84$, $P = 0.0004$; Fig. 8a, b). Further dendritic spine dynamics analysis indicated that SR33557 reversed the decrease of mushroom spines and the increase of stubby spines induced by sortilin overexpression but did not influence the thin spines in the prefrontal cortex ($F_{4,27} = 13.83$, $P < 0.0001$; Fig. 8a). In the hippocampus, SR33557 reversed the decrease of mushroom spines and the increase of stubby spines and thin spines induced by sortilin overexpression ($F_{4,27} = 46.72$, $P < 0.0001$; Fig. 8b). Western blot analysis showed that SR33557 reversed the PSD95 and SYP38 downregulation induced by sortilin overexpression in the prefrontal cortex ($F_{2,15} = 11.86$, $P = 0.0008$ and $F_{2,15} = 29.98$, $P < 0.0001$, respectively; Fig. 8c) and hippocampus ($F_{2,15} = 53.09$, $P < 0.0001$ and $F_{2,15} = 19.22$, $P < 0.0001$, respectively; Fig. 8d). Next, changes in the RhoA/ROCK2-signaling pathway were examined. Western blot analysis showed that SR33557 significantly reversed the increased ROCK2 levels ($F_{2,12} = 17.82$, $P = 0.0003$ and $F_{2,12} = 19.13$, $P = 0.0002$, respectively; Fig. 8e, f) and the decreased cofilin phosphorylation levels ($F_{2,15} = 18.41$, $P < 0.0001$ and $F_{2,15} = 40.04$, $P < 0.0001$, respectively; Fig. 8g, h) caused by sortilin overexpression in the prefrontal cortex and hippocampus. The results indicated that SR33557 influences the regulation of sortilin in the RhoA/ROCK2 signaling pathway. In summary, these results indicated that sortilin regulates the activation of RhoA/ROCK2 signaling and the loss of dendritic spines via ASM/ceramide signaling in depressive disorders.

DISCUSSION

Sortilin is widely expressed in the brain. In the mature mouse brain, sortilin expression occurs widely in the cerebellum, diencephalon, subpallium, cerebral cortex, and hippocampus [42]. However, no dedicated research has investigated the physiological roles of sortilin in different brain regions. Sortilin has been thought to play essentially similar physiological roles in different brain regions, involving the intracellular sorting and trafficking of various proteinic substrates between the TGN and plasma membrane compartments [43]. Thus, sortilin acts as a receptor or co-receptor to bind extracellular ligands, facilitating

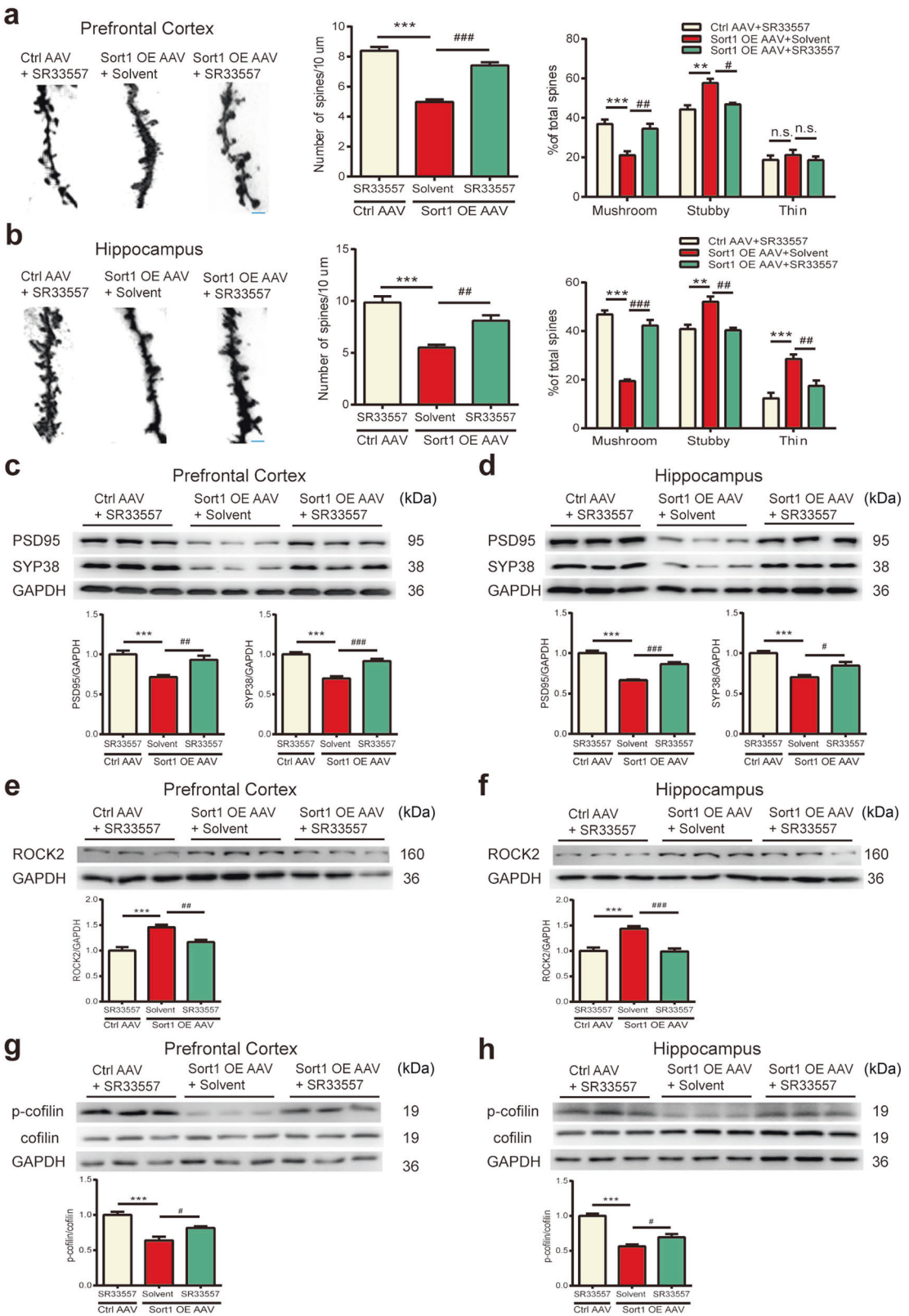

Fig. 8 Repression of ASM reverses loss of dendritic spines induced by sortilin overexpression. a, **b** Representative images of Golgi staining for dendritic spines and quantitative analysis of dendritic spine dynamics in the PFC (**a**) and Hipp (**b**) of mice. $n = 4$–5 per group. Scale bars = 2 μm. **c**, **d** Western blot analysis of SYP38 and PSD95 expression in the PFC (**c**) and Hipp (**d**) of mice. $n = 4$ per group. **e**, **f** Western blot analysis of ROCK2 expression in the PFC (**e**) and Hipp (**f**) of mice. $n = 4$ per group. **g**, **h** Western blot analysis of phosphorylation levels of cofilin in the PFC (**g**) and Hipp (**h**) of mice. $n = 4$ per group. $^{*}P < 0.05$, $^{**}P < 0.01$, $^{***}P < 0.001$ compared with Ctrl AAV + SR33557; $^{\#}P < 0.05$, $^{\#\#}P < 0.01$, $^{\#\#\#}P < 0.001$ compared with Sort1 OE AAV + Solvent. One-way ANOVA, Holm–Sidak's multiple comparisons test. All data are represented as mean ± SEM.

signaling or receptor-mediated endocytosis under specific conditions. The most important physiological role of sortilin in the brain is controlling (pro)-neurotrophin signaling, which ultimately mediates the survival, growth, differentiation, and apoptosis of neurons [16, 44, 45]. One study showed that sortilin binds APOE/Aβ complexes to mediate its clearance pathway, which plays a key role in Alzheimer's disease [17]. Another study showed that sortilin binds with progranulin protein, resulting in cellular uptake and degradation of the protein, which ultimately influences frontotemporal lobar degeneration [12].

The common mechanism of MDD is complex. The main accepted pathological mechanisms of MDD are hereditary factors, changes in neurotransmitter systems, absence of brain-derived neurotrophic factor (BDNF), hypothalamic–pituitary–adrenal axis dysfunction, increased inflammatory molecule expression, energy metabolism disorder, and synapse structure abnormality [46]. A previous study of the relationship between sortilin and MDD reported that sortilin upregulation was accompanied by BDNF downregulation in the serum of MDD patients [20]. The administration of electroconvulsive therapy to MDD patients has been found to ameliorate depressive-like symptoms, accompanied by serum sortilin downregulation [47]. Another study found that sortilin-deficient mice showed reduced TREK-1 expression, which indirectly led to an increase in 5-HT neuronal firing activity, and increased levels of BDNF and the BDNF-activated receptor TrkB [22]. These results suggest that sortilin is related to changes in neurotransmitter systems and the BDNF pathological mechanism of MDD.

It is widely accepted that exposing mice to stress simulates the pathogenesis of MDD [48, 49]. In the present study, we used CUMS, a common chronic stress model, to explore the underlying mechanism of MDD. Some studies have reported that sortilin is closely associated with clinical and preclinical depression [21, 22]. However, whether sortilin plays a positive or negative regulatory role in depression remains controversial, and the specific mechanism by which sortilin regulates depression is unknown. In this study, we determined that sortilin in the prefrontal cortex and hippocampus plays a pivotal role in depression. Our results showed that after 6 weeks of CUMS, sortilin was highly expressed in the prefrontal cortex and hippocampus, but not in the nucleus accumbens and amygdala. By examining differential sortilin expression in different brain regions of depressive-like mice, we focused on the role of sortilin in the prefrontal cortex and hippocampus of these mice. However, we were unable to determine whether sortilin had any effect on the nucleus accumbens or amygdala in depression. In contrast with our results, two independent studies reported that sortilin knockout mice displayed no obvious depressive-like behaviors [22, 23], which suggests that sortilin may play various roles in different brain regions. Therefore, future studies should determine the specific contribution of sortilin to depression in each brain region.

Based on the changes of sortilin in the prefrontal cortex and hippocampus in CUMS mice, how sortilin in the two brain regions participated in depressive disorders was investigated. First, AAV9-Sort1-shRNA was stereotaxically injected into the prefrontal cortex and hippocampus of mice to cause knockdown of sortilin in the two regions. Results from behavioral tests showed that specific knockdown of sortilin had no effect on depression-related behaviors of stress-naive mice but could improve the depressive-like behaviors of CUMS mice. Next, AAV9-Sort1 was stereotaxically injected into the prefrontal cortex and hippocampus of mice to overexpress sortilin in these two regions; sortilin overexpression in the prefrontal cortex and hippocampus was sufficient to induce depression directly without undergoing CUMS. Therefore, sortilin in the prefrontal cortex and hippocampus participates in the pathogenesis of depression. However, whether sortilin in other depression-related brain regions, such as the nucleus accumbens and amygdala, is involved in depression remains unknown.

Based on the behavior test results, the mechanism by which sortilin in the prefrontal cortex and hippocampus mediates depressive disorders was investigated. The ASM/ceramide abnormality hypothesis, which posits that the abnormal enhancement of ASM enzyme activity leads to overproduction of various forms of ceramides in depression [36, 50], has recently attracted increased attention. In a previous study, sortilin was shown to mediate ASM transport and maturation within cells [24]. Therefore, we investigated the mechanism by which sortilin affects ASM/ceramide signaling in the present study. Specific knockdown of sortilin reduced ASM enzyme activity and total ceramide levels in mice subjected to CUMS, including stress-naive mice. Conversely, specific overexpression of sortilin increased ASM enzyme activity and total ceramide levels. Further experiments showed that sortilin promoted ASM trafficking from the TGN to the lysosome, where it is activated and catalyzes sphingomyelin into multiple forms of ceramides. Significant inhibition of ASM activity may cause side effects, because normal ASM activity is important for maintaining internal homeostasis. To inhibit ASM activity, we used an ASM inhibitor and AAV9-Sort1-shRNA in the present study, and observed no apparent influence on depressive-like behaviors in stress-naive mice. Among the behavior tests, the OFT, FST, and TST showed that the inhibition of ASM did not induce manic behaviors. In summary, the results indicated that the inhibition of ASM activity had no significant side effects and could ameliorate depressive-like behaviors in mice. Therefore, intervening in ASM activity may become a potential treatment option for MDD.

As downstream molecules of the sortilin–ASM axis, ceramides have a variety of physiological functions. Ceramides are mainly located in cell membranes and have a regulatory function in cell survival and proliferation [51], differentiation [52], and apoptosis [53]. Because numerous forms of ceramides are closely associated with MDD [35], we used a total ceramide ELISA kit to detect total ceramide levels. However, the mechanism by which ceramides induce depression remains unknown.

Increasing evidence indicates that structural synapse changes and protein content alteration occur in depression pathophysiology. A postmortem report showed that the number of synapses in the dorsolateral prefrontal cortex was significantly decreased in MDD patients [54]. In a CUMS mouse model, reduced neuronal synapse quantity was observed in the prefrontal cortex and CA3 subregion of the hippocampus [55]. Aberrant synapse structure and number tend to impair synaptic plasticity and neural circuits between different brain areas of the limbic system, and are responsible for depression symptoms [56, 57]. The results of the present study showed that specific sortilin regulation altered the number and type of dendritic spines. Specific knockdown of sortilin restored dendritic spine loss induced by CUMS; however, the ASM inhibitor also restored the loss of dendritic spines induced by specific sortilin overexpression, indicating that sortilin regulates ASM/ceramide signaling to affect the number of dendritic spines. CUMS decreased the prevalence of mushroom-shaped dendritic spines and increased that of thin dendritic spines, thereby converting more mature dendrites to the immature type. However, specific knockdown of sortilin reversed this situation. Stubby dendritic spines, which are usually considered to be a transitional form of dendritic spine during maturation, did not change in number under CUMS or sortilin knockdown conditions.

Among numerous theories explaining the abnormality of dendritic spines in depression [58–60], we hypothesized that RhoA/ROCK signaling is regulated by ceramides. The results of the present study verified our hypothesis. Specific sortilin knockdown reversed CUMS-induced hyperactivity of RhoA and ROCK2, affecting phosphorylation levels of the key downstream molecule cofilin. In a previous report, cofilin phosphorylation was shown to be important for regulating dendritic spine dynamics [31].

Activated RhoA and ROCK2 inhibit cofilin phosphorylation, and low cofilin phosphorylation levels are insufficient to stabilize dendritic spine structure, leading to dendritic spine loss [61]. To confirm the relationship between ASM/ceramide and RhoA/ROCK2 signaling, we applied the ASM inhibitor SR33557, which reversed the ROCK2 expression and cofilin phosphorylation induced by specific sortilin overexpression. These results confirmed the involvement of the sortilin–ASM–ceramide axis in regulating dendritic spine dynamics via RhoA/ROCK2 signaling in the prefrontal cortex and hippocampus of CUMS mice. SR33557 also showed significant effects on depressive-like behaviors; we speculate that these effects are mainly due to the importance of ASM in depression pathology. A previous study showed that ASM enzyme activity was highly expressed in MDD patients [33], and that antidepressants such as amitriptyline and fluoxetine ameliorate depressive-like behaviors through the inhibition of ASM enzyme activity [30, 62]. A few explanations of the mechanism of ASM's role in depression pathology have been proposed. One study showed that therapeutic concentrations of two antidepressants (amitriptyline and fluoxetine) reduced ASM activity and ceramide concentrations in the hippocampus, increased neuronal proliferation, maturation, and survival, and improved behavior in stress-induced mice [30]. Another study showed that ASM inhibition by amitriptyline prevented stress-induced phosphorylation of p38 MAPK, thereby rescuing reduced neurogenesis and ameliorating depressive-like symptoms [62]. These studies demonstrate that ASM plays an important role in depression pathogenesis and that the underlying mechanisms are very broad.

In conclusion, the findings of our study demonstrate that specific knockdown of sortilin in the prefrontal cortex and hippocampus mitigates depressive-like behaviors induced by CUMS, providing direct evidence that sortilin signaling mediates the pathology of depression. Further experiments showed that sortilin in the prefrontal cortex and hippocampus regulates depressive-like behaviors induced by CUMS via ASM–ceramide–RhoA/ROCK2 signaling to affect dendritic spine dynamics. Overall, the results of the present study indicate that sortilin is a potential new target for MDD therapeutics.

ACKNOWLEDGEMENTS

This work was supported by grants of National Natural Science Foundation of China (81772063, 82073831), Natural Science Foundation of Jiangsu Province (BK20191325), and "Double First-Class" University project (CPU2018GY20, CPU2018GY13) to HL.

AUTHOR CONTRIBUTIONS

HL and SJC conceived and designed the research; SJC, CCG, and MQZ performed experiments; SJC and CCG analyzed data; HL, SJC, QYL, CCG, and XYQ wrote the manuscript. All authors reviewed and approved the final version of the manuscript.

ADDITIONAL INFORMATION

Supplementary information The online version contains supplementary material available at https://doi.org/10.1038/s41401-021-00823-0.

Competing interests: The authors declare no competing interests.

REFERENCES

1. Dean J, Keshavan M. The neurobiology of depression: an integrated view. Asian J Psychiatr. 2017;27:101–11.
2. Smith K. Mental health: a world of depression. Nature. 2014;515:181.
3. Petersen CM, Nielsen MS, Nykjaer A, Jacobsen L, Tommerup N, Rasmussen HH, et al. Molecular identification of a novel candidate sorting receptor purified from human brain by receptor-associated protein affinity chromatography. J Biol Chem. 1997;272:3599–605.
4. Sarret P, Krzywkowski P, Segal L, Nielsen MS, Petersen CM, Mazella J, et al. Distribution of NTS3 receptor/sortilin mRNA and protein in the rat central nervous system. J Comp Neurol. 2003;461:483–505.
5. Mazella J, Zsurger N, Navarro V, Chabry J, Kaghad M, Caput D, et al. The 100-kDa neurotensin receptor is gp95/sortilin, a non-G-protein-coupled receptor. J Biol Chem. 1998;273:26273–6.
6. Munck Petersen C, Nielsen MS, Jacobsen C, Tauris J, Jacobsen L, Gliemann J, et al. Propeptide cleavage conditions sortilin/neurotensin receptor-3 for ligand binding. EMBO J. 1999;18:595–604.
7. Nykjaer A, Lee R, Teng KK, Jansen P, Madsen P, Nielsen MS, et al. Sortilin is essential for proNGF-induced neuronal cell death. Nature. 2004;427:843–8.
8. Evans SF, Irmady K, Ostrow K, Kim T, Nykjaer A, Saftig P, et al. Neuronal brain-derived neurotrophic factor is synthesized in excess, with levels regulated by sortilin-mediated trafficking and lysosomal degradation. J Biol Chem. 2011;286:29556–67.
9. Tang W, Lu Y, Tian QY, Zhang Y, Guo FJ, Liu GY, et al. The growth factor progranulin binds to TNF receptors and is therapeutic against inflammatory arthritis in mice. Science. 2011;332:478–84.
10. Mazella J, Petrault O, Lucas G, Deval E, Beraud-Dufour S, Gandin C, et al. Spadin, a sortilin-derived peptide, targeting rodent TREK-1 channels: a new concept in the antidepressant drug design. PLoS Biol. 2010;8:e1000355.
11. Canuel M, Korkidakis A, Konnyu K, Morales CR. Sortilin mediates the lysosomal targeting of cathepsins D and H. Biochem Biophys Res Commun. 2008;373:292–7.
12. Hu F, Padukkavidana T, Vaegter CB, Brady OA, Zheng Y, Mackenzie IR, et al. Sortilin-mediated endocytosis determines levels of the frontotemporal dementia protein, progranulin. Neuron. 2010;68:654–67.
13. Gustafsen C, Kjolby M, Nyegaard M, Mattheisen M, Lundhede J, Buttenschon H, et al. The hypercholesterolemia-risk gene SORT1 facilitates PCSK9 secretion. Cell Metab. 2014;19:310–8.
14. Bi L, Chiang JY, Ding WX, Dunn W, Roberts B, Li T. Saturated fatty acids activate ERK signaling to downregulate hepatic sortilin 1 in obese and diabetic mice. J Lipid Res. 2013;54:2754–62.
15. Kaddai V, Jager J, Gonzalez T, Najem-Lendom R, Bonnafous S, Tran A, et al. Involvement of TNF-alpha in abnormal adipocyte and muscle sortilin expression in obese mice and humans. Diabetologia. 2009;52:932–40.
16. Yang M, Lim Y, Li X, Zhong JH, Zhou XF. Precursor of brain-derived neurotrophic factor (proBDNF) forms a complex with Huntingtin-associated protein-1 (HAP1) and sortilin that modulates proBDNF trafficking, degradation, and processing. J Biol Chem. 2011;286:16272–84.
17. Carlo AS, Gustafsen C, Mastrobuoni G, Nielsen MS, Burgert T, Hartl D, et al. The pro-neurotrophin receptor sortilin is a major neuronal apolipoprotein E receptor for catabolism of amyloid-beta peptide in the brain. J Neurosci. 2013;33:358–70.
18. Lee WC, Almeida S, Prudencio M, Caulfield TR, Zhang YJ, Tay WM, et al. Targeted manipulation of the sortilin-progranulin axis rescues progranulin haploinsufficiency. Hum Mol Genet. 2014;23:1467–78.
19. Bellanger C, Dubanet L, Lise MC, Fauchais AL, Bordessoule D, Jauberteau MO, et al. Endogenous neurotrophins and Trk signaling in diffuse large B cell lymphoma cell lines are involved in sensitivity to rituximab-induced apoptosis. PLoS One. 2011;6:e27213.
20. Zhou L, Xiong J, Lim Y, Ruan Y, Huang C, Zhu Y, et al. Upregulation of blood proBDNF and its receptors in major depression. J Affect Disord. 2013;150:776–84.
21. Buttenschon HN, Demontis D, Kaas M, Elfving B, Molgaard S, Gustafsen C, et al. Increased serum levels of sortilin are associated with depression and correlated with BDNF and VEGF. Transl Psychiatry. 2015;5:e677.
22. Moreno S, Devader CM, Pietri M, Borsotto M, Heurteaux C, Mazella J. Altered Trek-1 function in sortilin deficient mice results in decreased depressive-like behavior. Front Pharmacol. 2018;9:863.
23. Ruan CS, Yang CR, Li JY, Luo HY, Bobrovskaya L, Zhou XF. Mice with Sort1 deficiency display normal cognition but elevated anxiety-like behavior. Exp Neurol. 2016;281:99–108.
24. Wahe A, Kasmapour B, Schmaderer C, Liebl D, Sandhoff K, Nykjaer A, et al. Golgi-to-phagosome transport of acid sphingomyelinase and prosaposin is mediated by sortilin. J Cell Sci. 2010;123:2502–11.
25. Sahu P, Mudgal J, Arora D, Kinra M, Mallik SB, Rao CM, et al. Cannabinoid receptor 2 activation mitigates lipopolysaccharide-induced neuroinflammation and sickness behavior in mice. Psychopharmacol (Berl). 2019;236:1829–38.
26. Can A, Dao DT, Terrillion CE, Piantadosi SC, Bhat S, Gould TD. The tail suspension test. J Vis Exp. 2012:e3769.
27. Jeong HJ, Yang SY, Kim HY, Kim NR, Jang JB, Kim HM. Chelidonic acid evokes antidepressant-like effect through the up-regulation of BDNF in forced swimming test. Exp Biol Med (Maywood). 2016;241:1559–67.
28. Apazoglou K, Farley S, Gorgievski V, Belzeaux R, Lopez JP, Grenier J, et al. Antidepressive effects of targeting ELK-1 signal transduction. Nat Med. 2018;24:591–7.
29. Deng XY, Xue JS, Li HY, Ma ZQ, Fu Q, Qu R, et al. Geraniol produces antidepressant-like effects in a chronic unpredictable mild stress mice model. Physiol Behav. 2015;152:264–71.

30. Gulbins E, Palmada M, Reichel M, Luth A, Bohmer C, Amato D, et al. Acid sphingomyelinase-ceramide system mediates effects of antidepressant drugs. Nat Med. 2013;19:934–8.
31. Pyronneau A, He Q, Hwang JY, Porch M, Contractor A, Zukin RS. Aberrant Rac1-cofilin signaling mediates defects in dendritic spines, synaptic function, and sensory perception in fragile X syndrome. Sci Signal. 2017;10:eaan0852.
32. Ma M, Ren Q, Yang C, Zhang JC, Yao W, Dong C, et al. Antidepressant effects of combination of brexpiprazole and fluoxetine on depression-like behavior and dendritic changes in mice after inflammation. Psychopharmacology (Berl). 2017;234:525–33.
33. Kornhuber J, Medlin A, Bleich S, Jendrossek V, Henkel AW, Wiltfang J, et al. High activity of acid sphingomyelinase in major depression. J Neural Transm (Vienna). 2005;112:1583–90.
34. Kornhuber J, Reichel M, Tripal P, Groemer TW, Henkel AW, Muhle C, et al. The role of ceramide in major depressive disorder. Eur Arch Psychiatry Clin Neurosci. 2009;259(Suppl 2):S199–204.
35. Dinoff A, Herrmann N, Lanctot KL. Ceramides and depression: a systematic review. J Affect Disord. 2017;213:35–43.
36. Gulbins E, Walter S, Becker KA, Halmer R, Liu Y, Reichel M, et al. A central role for the acid sphingomyelinase/ceramide system in neurogenesis and major depression. J Neurochem. 2015;134:183–92.
37. Hubel E, Saroha A, Park WJ, Pewzner-Jung Y, Lavoie EG, Futerman AH, et al. Sortilin deficiency reduces ductular reaction, hepatocyte apoptosis, and liver fibrosis in cholestatic-induced liver injury. Am J Pathol. 2017;187:122–33.
38. Fox ME, Chandra R, Menken MS, Larkin EJ, Nam H, Engeln M, et al. Dendritic remodeling of D1 neurons by RhoA/Rho-kinase mediates depression-like behavior. Mol Psychiatry. 2020;25:1022–34.
39. Lu Y, Sun G, Yang F, Guan Z, Zhang Z, Zhao J, et al. Baicalin regulates depression behavior in mice exposed to chronic mild stress via the Rac/LIMK/cofilin pathway. Biomed Pharmacother. 2019;116:109054.
40. Li B, Xu Y, Quan Y, Cai Q, Le Y, Ma T, et al. Inhibition of RhoA/ROCK pathway in the early stage of hypoxia ameliorates depression in mice via protecting myelin sheath. ACS Chem Neurosci. 2020;11:2705–16.
41. Koch JC, Tonges L, Barski E, Michel U, Bahr M, Lingor P. ROCK2 is a major regulator of axonal degeneration, neuronal death and axonal regeneration in the CNS. Cell Death Dis. 2014;5:e1225.
42. Boggild S, Molgaard S, Glerup S, Nyengaard JR. Highly segregated localization of the functionally related vps10p receptors sortilin and SorCS2 during neurodevelopment. J Comp Neurol. 2018;526:1267–86.
43. Lv YC, Gao AB, Yang J, Zhong LY, Jia B, Ouyang SH, et al. Long-term adenosine A1 receptor activation-induced sortilin expression promotes alpha-synuclein upregulation in dopaminergic neurons. Neural Regen Res. 2020;15:712–23.
44. Chen ZY, Ieraci A, Teng H, Dall H, Meng CX, Herrera DG, et al. Sortilin controls intracellular sorting of brain-derived neurotrophic factor to the regulated secretory pathway. J Neurosci. 2005;25:6156–66.
45. Vaegter CB, Jansen P, Fjorback AW, Glerup S, Skeldal S, Kjolby M, et al. Sortilin associates with Trk receptors to enhance anterograde transport and neurotrophin signaling. Nat Neurosci. 2011;14:54–61.
46. Peng GJ, Tian JS, Gao XX, Zhou YZ, Qin XM. Research on the pathological mechanism and drug treatment mechanism of depression. Curr Neuropharmacol. 2015;13:514–23.
47. Stelzhammer V, Guest PC, Rothermundt M, Sondermann C, Michael N, Schwarz E, et al. Electroconvulsive therapy exerts mainly acute molecular changes in serum of major depressive disorder patients. Eur Neuropsychopharmacol. 2013;23:1199–207.
48. Nollet M, Le Guisquet AM, Belzung C. Models of depression: unpredictable chronic mild stress in mice. Curr Protoc Pharmacol. 2013;Chapter 5:Unit 5.65.
49. Planchez B, Surget A, Belzung C. Animal models of major depression: drawbacks and challenges. J Neural Transm (Vienna). 2019;126:1383–408.
50. Kornhuber J, Muller CP, Becker KA, Reichel M, Gulbins E. The ceramide system as a novel antidepressant target. Trends Pharmacol Sci. 2014;35:293–304.
51. Olivera A, Romanowski A, Rani CS, Spiegel S. Differential effects of sphingomyelinase and cell-permeable ceramide analogs on proliferation of Swiss 3T3 fibroblasts. Biochim Biophys Acta. 1997;1348:311–23.
52. Okazaki T, Bell RM, Hannun YA. Sphingomyelin turnover induced by vitamin D3 in HL-60 cells. Role in cell differentiation. J Biol Chem. 1989;264:19076–80.
53. Huang Y, Wu S, Zhang Y, Zi Y, Yang M, Guo Y. et al. [Ceramide participates in cell programmed death induced by Type II anti-CD20 mAb]. Zhong Nan Da Xue Xue Bao Yi Xue Ban. 2015;40:1292–7.
54. Wang Q, Timberlake MA II, Prall K, Dwivedi Y. The recent progress in animal models of depression. Prog Neuropsychopharmacol Biol Psychiatry. 2017;77:99–109.
55. Trivedi MH, Rush AJ, Wisniewski SR, Nierenberg AA, Warden D, Ritz L, et al. Evaluation of outcomes with citalopram for depression using measurement-based care in STAR*D: implications for clinical practice. Am J Psychiatry. 2006;163:28–40.
56. Kang HJ, Voleti B, Hajszan T, Rajkowska G, Stockmeier CA, Licznerski P, et al. Decreased expression of synapse-related genes and loss of synapses in major depressive disorder. Nat Med. 2012;18:1413–7.
57. Duman RS, Aghajanian GK. Synaptic dysfunction in depression: potential therapeutic targets. Science. 2012;338:68–72.
58. Qiao H, Li MX, Xu C, Chen HB, An SC, Ma XM. Dendritic spines in depression: what we learned from animal models. Neural Plast. 2016;2016:8056370.
59. Qu Y, Yang C, Ren Q, Ma M, Dong C, Hashimoto K. Regional differences in dendritic spine density confer resilience to chronic social defeat stress. Acta Neuropsychiatr. 2018;30:117–22.
60. Zhu XL, Chen JJ, Han F, Pan C, Zhuang TT, Cai YF, et al. Novel antidepressant effects of Paeonol alleviate neuronal injury with concomitant alterations in BDNF, Rac1 and RhoA levels in chronic unpredictable mild stress rats. Psychopharmacology (Berl). 2018;235:2177–91.
61. Garcia-Rojo G, Fresno C, Vilches N, Diaz-Veliz G, Mora S, Aguayo F, et al. The ROCK inhibitor fasudil prevents chronic restraint stress-induced depressive-like behaviors and dendritic spine loss in rat hippocampus. Int J Neuropsychopharmacol. 2017;20:336–45.
62. Grassme H, Jernigan PL, Hoehn RS, Wilker B, Soddemann M, Edwards MJ, et al. Inhibition of acid sphingomyelinase by antidepressants counteracts stress-induced activation of P38-kinase in major depression. Neurosignals. 2015;23:84–92.